Energy and exergy analysis of negative CO_2 emission gas power plant operation using thermodynamic modelling results of the cycle

Paweł MADEJSKI[1#]*, Ivar S. ERTESVÅG[2], Paweł ZIÓŁKOWSKI[3], Dariusz MIKIELEWICZ[3]

[1] *AGH University of Science and Technology, Faculty of Mechanical Engineering and Robotics, Al. Mickiewicza 30, 30-059 Kraków, Poland*

[2]*NTNU Norwegian University of Science and Technology, Department of Energy and Process Engineering, Kolbjørn Hejes v 1B, NO-7491 Trondheim, Norway*

[3] *Gdańsk University of Technology, Faculty of Mechanical Engineering and Ship Technology, Gabriela Narutowicza Str. 11/12, 80-233 Gdańsk, Poland*

**Corresponding Author, pawel.madejski@agh.edu.pl, [#]Presenting Author*

Abstract – A developed cycle of negative CO_2 emission gas power plant is presented. The cycle is an oxy-combustion gas turbine cycle where the gas fuel is burnt with pure oxygen, and liquid water is injected to the combustor to keep the temperature at an appropriate level for the gas turbine. The negative level of CO_2 emission can be obtained by combining CO_2 capture method with the usage of a gas fuel based on sewage sludge gasification. This fuel is regarded as a biomass fuel with zero emission of CO_2. First, the paper presents modeling results of the basic cycle fired with syngas from sewage sludge. For comparison, the cycle is also simulated with methane as the fuel. Energy and exergy analyses of the cycle are conducted. They show the impact of the input values on the total energy and exergy efficiency and on exergy destruction in the cycle components. Next, the presented cycle based on the combustion in the oxygen atmosphere is developed by adding part of the oxy-combustion CO_2 capture method using a direct-contact heat exchanger to condensate steam and separate CO_2. The energy and exergy calculation results give a chance to compare the results of the developed cycle with the cycle when the natural gas (methane) is used as the primary gas fuel. In an exergy analysis, the initial state is specified as the input values for the gas fuel, oxygen, and water and is equal to 15° C and 1 bar. The energy and exergy balance calculations were conducted using developed thermodynamic models of the cycles. Calculation of the main cycle parameter as power output, heat, fuel consumption, and indicators such as the total energy efficiency, total exergy efficiency, heat rate, etc., gives the opportunity to evaluate the developed cycle and indicate components where the most significant losses can occur. The analysis shows that the process of water injection can give somewhat higher exergy destruction in the combustor compared with conventional gas turbine combustors; approximately 45% versus 35%. Furthermore, the chemical exergy of the captured CO_2 represents 3.3% of the fuel chemical exergy for syngas, while 2.2% for methane. This is the thermodynamic value of the capture. Results of analysis will be helpful in the process design of the negative CO_2 emission gas power plant cycle concept.

1 Introduction

The background of this work is twofold: First, handling of sewage sludge poses a considerable environmental challenge to urban societies. Second, CO_2 emissions contribute to global warming. Sewage sludge is biomass and can be converted to combustible gases to fuel a thermal power plant. If an oxy-combustion (aka. oxy-fuel) technology is used, the produced CO_2 can be sequestered and stored, to avoid CO_2 emissions. As biomass (here sewage) is regarded carbon neutral, the sequestering makes the plant CO_2 negative.

The present paper is part of a project nCO2PP [1], aiming at realizing a negative CO_2 power plant. The process has been presented previously [2], with mass and energy analysis. Here, an exergy analysis (1st and 2nd law analysis) will be conducted and presented.

The developed cycle consists of innovative components such as a Wet combustion Chamber WCC, Spray Ejector Condenser SEC with water/CO_2 separator designed and developed under the project nCO2PP [1].

The energy analysis performed [2] based on the thermodynamic modeling results allows to evaluate the overall process efficiency, taking into account the internal efficiency of individual cycle components. The exergy analysis results give new insight into the comprehensive process analysis by identifying and quantifying the thermodynamic losses and deficiencies of the process. Thereby, dedicated actions to improve the process can be made.

For mature technical systems, like the conventional gas-turbine cycle, the effective actions for improvement are usually well known by the relevant industry. However, for new solutions, like those presented here, the improvement potentials are not known and may not be obvious in the first place. For such systems, exergy analysis provides useful insight into the thermodynamic losses and, hence, the possibilities for improvement.

An example can be found in [3], where optimum operating parameters were determined based on exergy analyses with emphasis on the economics and emissions of the unit. Another example is combined cycle units with steam injection [4], where a two-pressure hear recovery steam generator was analyzed, showing that there is a definite relationship between the amount of steam injected into the combustion chamber and the air flowing in the nominal state, when the highest energy and exergy efficiencies are achieved. Another solution is to make the CCGT cogeneration unit more flexible for different types of retrofits, which was performed for the unit in Gorzów Wielkopolski, where two types of steam injection into the combustion chamber, STIG and CSTIG, were analyzed [5]. It was shown that higher exergy losses in the combustion chamber occur for the STIG solution, but it is also more flexible. Of course, there are optimisations in the literature for gas turbines alone [6][7], but a much broader range of analyses needs to be carried out for CCGT units that aim to capture carbon dioxide. Here, we traditionally distinguish between three technologies, namely post-combustion [8][9], pre-combustion [10] and oxy-combustion [11][12]. Detailed exergetic analyses for several cases of CO_2 capture by chemical absorption and CO_2 compression systems were presented in [8], and a configuration was obtained in which the exergetic losses were at the lowest level with simultaneous preparation of CO_2 for sequestration. Also systems in which pre-combustion occurs should be analysed exergetically because surprising results can be obtained: for example, that the second most destructive exergy after the combustion chamber is the exchanger that cools the resulting

gas, because there may be an unfavourable temperature distribution in the device [10]. Such information provides a reliable basis for optimising the process and avoiding exergy losses to the environment. A system [11] with similarities to the one considered in the present paper concerns oxy-combustion, where the predominant role in the working medium is played by CO_2. The influences of two fundamental parameters on the increase in exergy destruction were been studied, namely: s-CO2-to-O_2 molar ratio (CtO) and in the primary zone and primary diluent ratio (PDR). The results confirmed that an increase in these parameters leads to an increase in exergy losses. In oxy-combustion, oxygen separation from air is an important sub-process, which was analyzed and optimized by exergy analysis by [13].

At this point, it is worth noting that in general, system zero-emissions can be achieved in two ways in combustion plants, namely: 1) burn fossil fuel and capture CO_2; 2) burn fuel from renewable sources, such as sewage sludge gasification. However, the combination of both techniques associated with syngas combustion and CO_2 capture will lead to a system with a negative carbon footprint. At the beginning, it should be said that in this study, due to the fact that the target fuel in the project is gas from gasification, two systems are distinguished. The first is zero-emission, where we burn syngas but do not capture CO_2 in equipment designed for this purpose. The second is a negative CO_2 cycle, where both the syngas from the gasification of sewage sludge is combusted and the resulting CO_2 is captured in a spray-ejector condenser with separator.

Therefore, for the sake of clarity of the message, it is worth distinguishing the two proposed processes shown in the following sections. First, the basic configuration proposal without CO_2 capture is discussed - a zero-CO_2 emission gas process (PFD0). In the second, the full version with CO_2 capture and compression (negative-CO_2 emission gas cycle (PFD1)) is presented. The following Section 3 describes the model prepared in Ebsilon and the basics of the exergetic analysis. The 4th section is a presentation of the results and a discussion of the analysis.

2 Negative CO_2 emission gas power plant using gasified sewage sludge

2.1 Basic oxy-combustion gas turbine process

The negative CO_2 emission gas power plant to be developed and investigated is based on gasification of sewage and combustion of the producer gas (aka. syngas) with pure oxygen (not air). To reduce the temperature of the combustion and of the resulting flue gases, liquid water is injected into the combustion chamber. Thus, it is a wet combustion chamber (WCC) in a water-cooled oxy-fuel combustion process. Due to the cost of O_2 production, the fuel-oxygen ratio has to be close to stoichiometric.

The basic oxy-combustion gas turbine process is shown in Figure 1 (cf. [2]). The flows of gas fuel (Stream 0^{fuel}) and oxygen (Stream 0^{O2}) are compressed in compressors C_{oxy} and C_{fuel} from the inlet pressures to combustor injection pressure and fed (Streams 1^{Fuel} and 1^{O2}) to the WCC. The inlet liquid water flow (Stream $0^{1\text{-}H2O}$) is pumped (pump P), heated in a recuperator (heat exchanger HE) and then injected (Stream 1^{H2O}) to the WCC. The fuel is burned with oxygen. Water is injected and evaporated to keep the temperature appropriate for the gas turbine. The flue gas (Stream 2) is expanded trough gas turbines GT1 and GT2, and then used to heat the

incoming water (HE). The gas turbines power the compressors, a pump and a generator, G. Assuming complete combustion with the stoichiometric air, the flue gas (Streams 2 to 5) consists of H_2O and CO_2, with a small amount of N_2 (from ammonia). The exhaust at a low pressure (Stream 5) is then ducted further to the spray ejection condenser (outside the process PFD0).

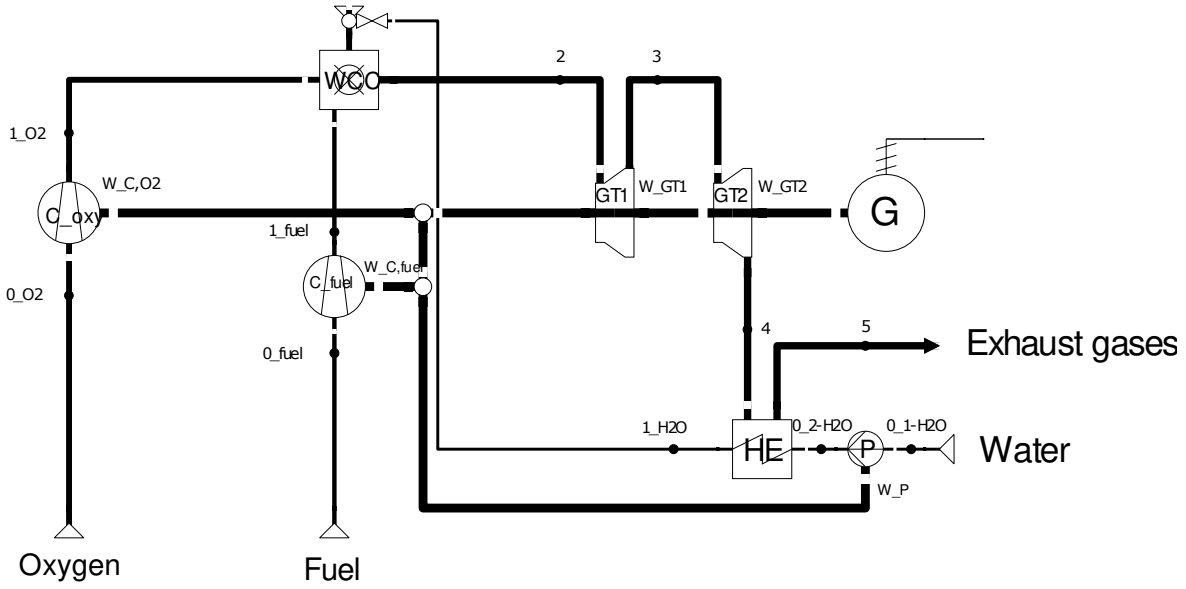

Figure 1: Process flow diagram of a zero-CO_2 emission gas process (PFD0)

2.2 Negative-CO_2 emission gas power cycle

The cycle based on the oxy-combustion gas turbine cycle above, extended by the CO_2 capture installation components, is presented in Figure 2 (see also [2]). The exhaust gases at the GT2 outlet (Stream 5) are ducted to the Spray Ejector Condenser (EC), whereby the steam is condensed by direct contact with the cold inlet water (Stream 1^{SEC}) delivered by the water pump (P_{EC}). The further step is cooling the mixture of water/CO_2 (Stream $2^{1\text{-}SEC}$) by heat exchange with a low-temperature cooling medium (Streams 1^{LTS} to 2^{LTS}) in heat exchanger HE2. Here (Stream $2^{2\text{-}SEC}$), a substantial part of the H2O condenses to liquid, which is separated (Stream 6) in a separator (S) and directed out of the system (Stream 1^{PROD}) or re-used for injection to the EC or the WCC and for cooling (HE4, HE3). The remaining CO_2 rich gas (Stream 1^{CCU}) is compressed ($C1_{CO2}$, $C2_{CO2}$) and cooled (HE3, HE4) before it is removed beyond the system boundary (Stream 5^{CCU}). Electric motors, M, runs the pump P_{EC} and the compressors $C1_{CO2}$, $C2_{CO2}$.

The presented cycle is based on combustion in an oxygen atmosphere, giving mainly CO_2 and water vapour. The CO_2 capture method to use a direct-contact heat exchanger to condensate steam and thereby separate CO_2. The use of this kind of CCS (Carbon Capture and Storage) installation provides a reduction of CO_2 emission below zero level.

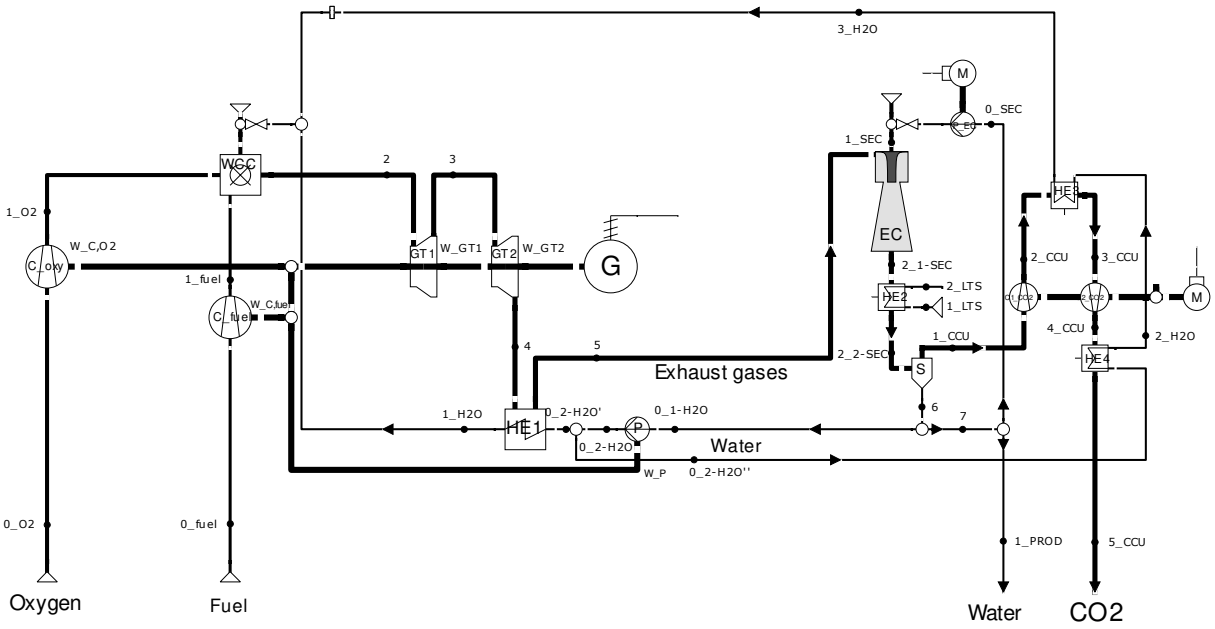

Figure 2: Process flow diagram of a negative-CO_2 emission gas cycle (PFD1)

2.3 Assumptions of the present predictions

The syngas mixture (aka. producer gas) from sewage sludge gasification [14] was assumed with a composition (molar based) of CO: 9.09%, CO_2: 25.61%, CH_4: 13.64%, C_3H_8: 3.39%, H_2: 45.16% and NH_3: 3.10%. In addition, for comparison, the process was also simulated with natural gas (simplified as pure CH_4) as the fuel.

For the calculations here, the ambient conditions (local atmosphere) were chosen as temperature $T_0 = 288.15$ K (15 °C), pressure $p_0 = 101325$ Pa (1 atm) and relative humidity $\varphi_0 = 0.60$.

The systems were assumed as steady-state steady-flow processes. Fuel, pure oxygen and pure water were assumed continuously available at the given inflow states. Each unit (subsystem) was assumed adiabatic. The combustion was assumed complete, converting all carbon to CO_2 and all hydrogen to H_2O. When relevant (syngas), fuel ammonia was assumed converted to N_2 and H_2O.

3 Thermodynamic modeling of zero-CO_2 and negative-CO_2 emission cycle

This section presents modeling results of the zero-CO_2 emission cycle and negative-CO_2 emission cycle fired with methane and syngas from sewage sludge gasification. The calculation results were obtained using a model developed in Ebsilon Professional software [15].

3.1 Model of zero-CO_2 emission gas power process

The model of the PFD0 process in Ebsilon professional is shown in Figure 3. The data shown for each flow (pressure, enthalpy, temperature, mass flow rate, exergy and "alternative exergy" from Ebsilon) are for the methane-fueled system.

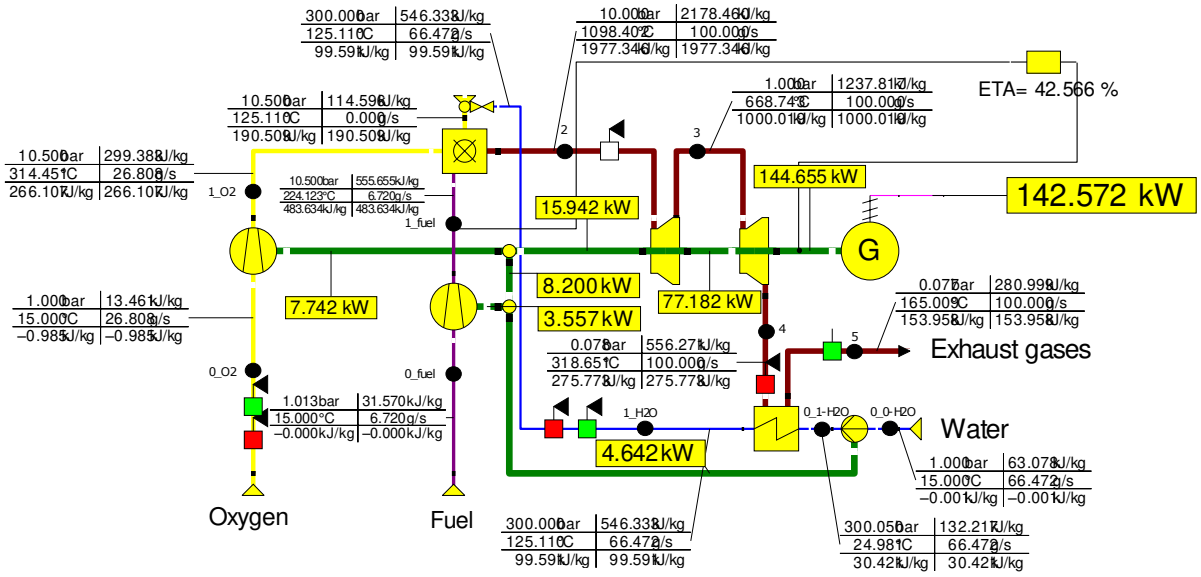

Figure 3: The developed thermodynamic model of the zero-CO2 emission process

3.2 Model of negative-CO_2 emission gas power cycle

In Figure 4 the power plant with CO_2 capture (PFD1) is shown. The data included in the graph is for methane fuel (pressure, enthalpy, temperature, mass flow rate, exergy and "alternative exergy" from Ebsilon). The PFD1 cycle model is an extension of the developed PFD0 process (Figure 3) by adding the components to simulate the operation of a spray ejector condenser (EC) with a water/gas separator (S), to capture and separate CO_2 from the exhaust gas. Model of spray ejector condenser uses input data of exhaust gas (pressure, mass flow rate), and pressure of motive water. The mass flow rate of motive fluid is calculated based on the correction factor for motive water flow. In the separator model assumption of full water liquid separation (water liquid separation rate equal to 1) was made. Models of other cycle components (compressor, pump, and heat exchanger) were adopted to calculate design size based on the input data of mass flow rate, temperature, and pressure data.

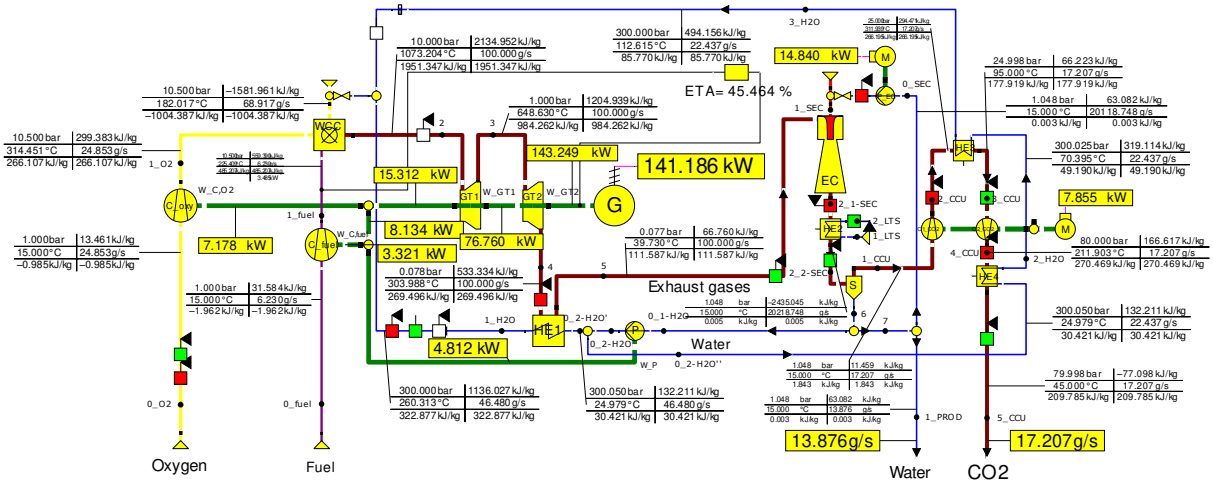

Figure 4: The developed thermodynamic model of the negative-CO2 emission gas power plant

3.3 Numerical simulation of gas power cycle using thermodynamic models

In the thermodynamic model, for gases, the Redlich-Kwong-Soave real gas formulation [16] is used, and for steam, the data of IPAWS-IF97 [17]. The equations of state, mass and energy balances are resolved iteratively, with a convergence criterion set to 10^{-9} (referring to the relative deviation between the second-last and the last iteration step for mass flow, pressure and enthalpy). The thermodynamic models of Ebsilon use the convention of setting the enthalpy zero point for gaseous flows like air and flue gas at 0°C. It can be noted that the enthalpy values displayed by Ebsilon do not balance for reactors and separators, i.e., when composition change. This affects postprocessing based on output quantities, while computations within the simulator seem to be correct.

3.4 Evaluation of exergy in flows of the power cycle using Ebsilon Professoinal

Flow exergy is the work theoretically obtainable when the flow is brought to total equilibrium with the environment. That is, in form of gases found in the stable atmosphere (N_2, O_2, H_2O, CO_2 and noble gases) at their respective partial pressures, $p_i^e = X_i^e p_0$, and at the temperature, T_0, in the ambient atmosphere. Here, X_i^e are the mole fractions of the gases in the atmosphere. The ambient conditions, or atmosphere, can be specified by specifying temperature (T_0), pressure (p_0),and relative humidity (φ_0) [18][19].

The flow exergy is customarily decomposed into a thermomechanical ("tm") part and chemical exergy. The latter is composed of a mixing part ("mix") and the component chemical exergies:

$$\dot{E}^{\mathrm{tot}} = \dot{E}^{\mathrm{tm}} + \dot{E}^{\mathrm{ch}} = \dot{H} - \dot{H}_0 - T_0\left(\dot{S} - \dot{S}_0\right) + \dot{E}^{\mathrm{mix}} + \sum\nolimits_i \dot{n}_i \overline{e}_i^{\mathrm{ch}} \tag{1}$$

Here $\dot{H}$ and $\dot{S}$ are the rates of enthalpy and entropy for the mixture, subscript 0 denotes that they are evaluated at the restricted dead state (T_0, p_0 for the mixture). Here, kinetic and potential energy are neglected. $\dot{n}_i$ and $\overline{e}_i^{\mathrm{ch}}$ are, respectively, the molar flow rate and the molar chemical exergy of species *i.*

The present study was based on the energy analysis conducted with the Ebsilon code. This software includes an exergy calculator. It evaluates the reversible work when the flow is brought from the actual state to the restricted dead state, that is (T_0, p_0), however not to the total equilibrium with the environment. Due to condensing and phase separation when this stream includes H_2O, the mixture is partly separated. This means that the Ebsilon exergy calculation includes a part of the mixing exergy, together with the thermomechanical component. The remaining part has to be evaluated when relevant. Thus, the total flow exergy rate can be evaluated as the quantity obtained from Ebsilon, here denoted $\dot{E}^{\mathrm{Ebs}}$, and the remaining part, which has to be calculated separately:

$$\dot{E}^{\mathrm{tot}} = \dot{E}^{\mathrm{Ebs}} + (\dot{E}^{\mathrm{tot}} - \dot{E}^{\mathrm{Ebs}}) \tag{2}$$

For a general flow containing H_2O (no other substances condensing at the relevant temperatures), the remaining part can be expressed as

$$(\dot{E}^{\text{tot}} - \dot{E}^{\text{Ebs}}) = T_0 \overline{R} \left(\sum_{i \neq \text{H}_2\text{O}} \dot{n}_i \ln X_{i0} + \underbrace{(\dot{n}_{\text{H}_2\text{O(g0)}} + \dot{n}_{\text{H}_2\text{O(liq0)}})}_{=\dot{n}_{\text{H}_2\text{O}}} \ln \frac{p_{s0}}{p_0} \right) + \\ + \dot{n}_{\text{H}_2\text{O(liq0)}} (p_0 - p_{s0}) \overline{v}_{\text{f}}(T_0) + \sum_i \dot{n}_i \overline{e}^{\text{ch}}_{i(g)} \tag{3}$$

Here, $\overline{R}$ is the universal gas constant, $\dot{n}_i$ is for the actual mixture. $\dot{n}_{\text{H}_2\text{O(g0)}}$ and $\dot{n}_{\text{H}_2\text{O(liq0)}}$ are, respectively, the mole fractions of, the molar flow rates of gaseous and liquid H_2O in the mixture when it is brought to the restricted dead state, while X_{i0} is the mole fraction for species *i* of the gaseous phase (non-condensed) at this state. These quantities are determined by setting the partial pressure of vapour H_2O equal to the saturation pressure at T_0 and by assuming that no gas is dissolved in the liquid. p_{s0} and $\overline{v}_{\text{f}}(T_0)$ are, respectively, the saturation pressure and saturated-liquid molar volume for H_2O at T_0. In the final term, it is emphasized that for H_2O, the component molar chemical exergy for gaseous state (g) is the relevant quantity in this expression (regardless of the phase of H_2O in the actual or restricted dead states).

For a flow without condensation at dead state, the expression simplifies to

$$(\dot{E}^{\text{tot}} - \dot{E}^{\text{Ebs}}) = T_0 \overline{R} \sum_i \dot{n}_i \ln X_i + \sum_i \dot{n}_i \overline{e}^{\text{ch}}_i \tag{4}$$

where the first right-hand side term is the mixing exergy of an ideal mixture. This term is negative, and it represents the exergy penalty of mixing the substances.

For the individual streams of the cycle, the exergy added to the Ebsilon exergy rate are as follows: For the fuel (assumed fully gaseous, no H_2O) and oxygen flows, the added exergy is simply the chemical exergy, comprising mixture exergy and component chemical exergies:

Methane (CH_4):

$$(\dot{E}^{\text{tot}} - \dot{E}^{\text{Ebs}}) = \dot{n}_{\text{CH}_4} \overline{e}^{\text{ch}}_{\text{CH}_4} \tag{5}$$

Syngas:

$$(\dot{E}^{\text{tot}} - \dot{E}^{\text{Ebs}}) = T_0 \overline{R} \sum_i \dot{n}_i \ln X_i + \sum_i \dot{n}_i \overline{e}^{\text{ch}}_i \\ = T_0 \overline{R} \left(\dot{n}_{\text{CO}} \ln \frac{\dot{n}_{\text{CO}}}{\dot{n}_{\text{total}}} + \dot{n}_{CO_2} \ln \frac{\dot{n}_{\text{CO}_2}}{\dot{n}_{\text{total}}} + \dot{n}_{\text{CH}_4} \ln \frac{\dot{n}_{\text{CH4}}}{\dot{n}_{\text{total}}} + \dot{n}_{\text{C}_3\text{H}_8} \ln \frac{\dot{n}_{\text{C}_3\text{H}_8}}{\dot{n}_{\text{total}}} + \dot{n}_{\text{H}_2} \ln \frac{\dot{n}_{\text{H}_2}}{\dot{n}_{\text{total}}} + \dot{n}_{\text{NH}_3} \ln \frac{\dot{n}_{\text{NH}_3}}{\dot{n}_{\text{total}}} \right) \\ + \dot{n}_{\text{CO}} \overline{e}^{\text{ch}}_{\text{CO}} + \dot{n}_{\text{CO}_2} \overline{e}^{\text{ch}}_{\text{CO}_2} + \dot{n}_{\text{CH}_4} \overline{e}^{\text{ch}}_{\text{CH}_4} + \dot{n}_{\text{C}_3\text{H}_8} \overline{e}^{\text{ch}}_{\text{C}_3\text{H}_8} + \dot{n}_{\text{H}_2} \overline{e}^{\text{ch}}_{\text{H}_2} + \dot{n}_{\text{NH}_3} \overline{e}^{\text{ch}}_{\text{NH}_3} \tag{6}$$

Oxygen:

$$(\dot{E}^{\text{tot}} - \dot{E}^{\text{Ebs}}) = \dot{n}_{\text{O}_2} \overline{e}^{\text{ch}}_{\text{O}_2} \tag{7}$$

Water: When this stream is liquid water only,

$$(\dot{E}^{\text{tot}} - \dot{E}^{\text{Ebs}}) = \dot{n}_{\text{H}_2\text{O,liq}} \overline{e}^{\text{ch}}_{\text{H}_2\text{O(liq)}} \tag{8}$$

while in general (vapour and/or liquid),

$$(\dot{E}^{\text{tot}} - \dot{E}^{\text{Ebs}}) = T_0 \overline{R} \left(\dot{n}_{\text{H}_2\text{O}} \ln \frac{p_{s0}}{p_0} \right) + \dot{n}_{\text{H}_2\text{O(liq0)}} (p_0 - p_{s0}) \overline{v}_{\text{f}}(T_0) + \dot{n}_{\text{H}_2\text{O}} \overline{e}^{\text{ch}}_{\text{H}_2\text{O(g)}} \tag{9}$$

The exhaust (flue gases)

$$\begin{aligned}(\dot{E}^{\text{tot}} - \dot{E}^{\text{Ebs}}) = T_0 \overline{R} \Bigg(& \dot{n}_{\text{CO}_2} \ln \frac{\dot{n}_{\text{CO}_2}}{\dot{n}_{\text{total}} - \dot{n}_{\text{H}_2\text{O(liq0)}}} + \dot{n}_{\text{N}_2} \ln \frac{\dot{n}_{\text{N}_2}}{\dot{n}_{\text{total}} - \dot{n}_{\text{H}_2\text{O(liq0)}}} + \dot{n}_{\text{H}_2\text{O}} \ln \frac{p_{s0}}{p_0} \Bigg) \\ & + \dot{n}_{\text{H}_2\text{O(liq0)}} (p_0 - p_{s0}) \overline{v}_{\text{f}}(T_0) + \dot{n}_{\text{CO}_2} \overline{e}^{\text{ch}}_{CO_2} + \dot{n}_{\text{H}_2\text{O}} \overline{e}^{\text{ch}}_{\text{H}_2\text{O(g)}} + \dot{n}_{\text{N}_2} \overline{e}^{\text{ch}}_{\text{N}_2}\end{aligned} \tag{10}$$

Here it is noted that for CH_4 as fuel, the flue-gas consists of CO_2 and H_2O (no N_2), while the syngas contains some NH_3 that reacts to N_2 (and H_2O).

The chosen ambient temperature (15 °C) corresponded to $p_{s0} = 1705.7$ Pa *and* $v_{\text{f}}(T_0) = 0.001000946\ \text{m}^3/\text{kg}$ *[17]. The molar volume is obtained with the molar mass:* $\overline{v}_{\text{f}}(T_0) = v_{\text{f}}(T_0) \cdot M_{\text{H}_2\text{O}}$. *The chemical exergies for the ambient conditions were evaluated with the model of [18] and presented in*

Table 1. The syngas fuel mixture had a chemical exergy of 331487 kJ/kmol (mixture exergy included), while the flue gas mixtures had values of 11034 kJ/kmol for syngas fuel and 10985 kJ/kmol for methane when no H_2O had condensed.

Table 1 : Chemical exergy for the pure components relevant for this study, evaluated at the chosen ambient conditions (15 °C, 1 atm, 60% RH).

Species	N_2	O_2	CO_2	H_2O(g)	H_2O(liq)
$\overline{e}^{\text{ch}}_i$ (kJ/kmol)	617	3769.99	18923.76	11010.11	1224
Species	H_2	CO	CH_4	C_3H_8	NH_3
$\overline{e}^{\text{ch}}_i$ (kJ/kmol)	238157	275131	834227	2154890	343289

3.5 Oxygen separation, carbon dioxide capture, exergy discharge

The pure O_2 used in oxy-combustion comes with a cost. The chemical exergy of the pure species constitutes the minimum thermodynamic requirement to produce it from the environment, i.e. the atmosphere. The actual requirement is higher. Based on the data observed in [2] and comparable to other data [13], the specific power consumption was set to 0.248 kWh/kgO_2. This corresponds to 28454 kJ/kmol, which is 7.55 times the chemical exergy.

In other words, the separation process has an efficiency of 13.2%. The required power, or exergy penalty, of the separation has to be subtracted from the gross power production of the power plant.

The flow of captured and compressed CO_2 is a desired product of the process. The exergy is the thermodynamic value of the flow. It therefore represents a useful product of the process,

along with the net power output. The chemical exergy of the product CO_2 is 2.2% of the chemical exergy of methane, while 3.3% for syngas. Thermomechanical exergy adds to these figures.

Most of the injected water is recirculated. The mass flow rate of water in the cycle is increased by the reaction product H_2O, which then is the net discharge. Its exergy is primarily the chemical exergy. Furthermore, some heat is discharged from heat exchanger HE2 by cooling water from the environment. In the present analysis, this discharge is accounted as part of the exergy destruction of the HE2. Indeed, some of this destruction is exergy discharged and then destructed in the environment. Nevertheless, it is a result of the process.

3.6 Energy and exergy analysis of the developed processes

For each unit (assumed steady state), the exergy balance was expressed as

$$0 = \sum_j (\dot{E}_j^{\text{tot}})_{\text{in}} - \sum_j (\dot{E}_j^{\text{tot}})_{\text{out}} - \dot{W} - \dot{E}_d \tag{11}$$

Here, j denotes a stream identifier, "in" and "out" refers to inflow and outflow of the unit, $\dot{W}$ is the power (work rate) delivered by the unit and $\dot{E}_d$ is the exergy destruction rate. For units with diffuse heat losses, the corresponding exergy loss was included in the exergy destruction rate. The work rates were obtained in the energy analysis (enthalpy rate differences), while the flow exergy rates were obtained as described above. The exergy destruction then appears as the remaining quantity to resolve from the exergy balance.

4 Results and discussion

The results show the impact of the input values on the total energy and exergy efficiency and on the exergy destruction level in the cycle components. The exergy analysis identifies and quantifies the thermodynamic losses in the process. The energy and exergy calculation results give a chance to compare the results of the developed cycle with the cycle when the natural gas (methane) is used as the primary gas fuel. The energy and exergy balance calculations were conducted using developed thermodynamic models of the presented cycles. Determination of the main cycle parameter as power output, heat input, fuel consumption, and indicators such as the total energy efficiency, total exergy efficiency, heat rate, etc., allows for evaluating the developed cycle and indicating components where the most significant losses can occur.

Table 2 summarizes the total mass and molar flow rates of each stream for methane, and furthermore, the temperature, pressure and specific enthalpy (from Ebsilon, see comment at the end of Section 3.3 above) from the energy analysis of PFD0 cycle. The total molar exergy and the total exergy rates (Eq. (2)) are also shown. Table 3 shows the same data for syngas.

Table 2: Calculation results in characteristic stream points of zero-CO2 emission process with Methane

Stream	$\dot{m}$ (g/s)	$\dot{n}$ (mol/s)	T (°C)	p (bar)	h (kJ/kg)	$\overline{e}^{tot}$ (kJ/mol)	$\dot{E}^{tot}$ (kW)
0^{Fuel}	6.72	0.419	15.00	1.000	31.58	834.196	349.435
1^{Fuel}	6.72	0.419	225.41	10.500	559.39	842.011	352.709
0^{O2}	26.81	0.838	15.00	1.000	13.46	3.770	3.158
1^{O2}	26.81	0.838	314.45	10.500	299.38	12.285	10.292
$0^{1\text{-}H2O}$	66.47	3.690	15.00	1.000	63.08	1.325	4.888
$0^{2\text{-}H2O}$	66.47	3.690	24.98	300.050	132.22	1.873	6.910
1^{H2O}	66.47	3.690	125.11	300.000	546.33	3.119	11.508
2	100.00	4.946	1098.51	10.000	4217.83	42.791	211.661
3	100.00	4.946	668.83	1.000	3277.11	23.031	113.921
4	100.00	4.946	318.71	0.078	2595.50	8.388	41.490
5	100.00	4.946	165.07	0.077	2320.23	5.925	29.306

Table 3: Calculation results in characteristic stream points of zero-CO2 emission process with Syngas

Stream	$\dot{m}$ (g/s)	$\dot{n}$ (mol/s)	T (°C)	p (bar)	h (kJ/kg)	$\overline{e}^{tot}$ (kJ/mol)	$\dot{E}^{tot}$ (kW)
0^{Fuel}	18.00	0.950	15.0	1.000	25.62	331.46	314.956
1^{Fuel}	18.00	0.950	252.9	10.500	483.27	339.49	322.591
0^{O2}	22.40	0.700	15.0	1.000	13.46	3.77	2.639
1^{O2}	22.40	0.700	314.5	10.500	299.38	12.29	8.601
$0^{1\text{-}H2O}$	59.60	3.308	15.0	1.000	63.08	1.32	4.377
$0^{2\text{-}H2O}$	59.60	3.308	25.0	300.050	132.22	1.87	6.190
1^{H2O}	59.60	3.308	125.1	300.000	546.33	3.12	10.312
2	100.00	4.740	1079.4	10.000	3940.71	42.34	206.154
3	100.00	4.740	657.2	1.000	3051.00	22.83	113.671
4	100.00	4.740	313.2	0.078	2404.78	8.34	44.964
5	100.00	4.740	170.6	0.077	2157.98	6.03	34.018

Table 4 shows the total mass and molar flow rates of each stream of PFD1 cycle fueled with methane, together with the temperature, pressure and specific enthalpy from the energy analysis, total molar exergy and the total exergy rates (Eq. (2)). The corresponding data for syngas are shown in Table 5.

Table 4: Calculation results in characteristic stream points of negative-CO2 emission cycle with Methane

Stream	$\dot{m}$ (g/s)	$\dot{n}$ (mol/s)	T (°C)	p (bar)	h (kJ/kg)	$\overline{e}^{tot}$ (kJ/mol)	$\dot{E}^{tot}$ (kW)
			Methane				
0^{Fuel}	6.23	0.388	15.00	1.000	31.58	834.196	323.96
1^{Fuel}	6.23	0.388	225.41	10.500	559.39	842.011	326.99
0^{O2}	24.85	0.777	15.00	1.000	13.46	3.770	2.928
1^{O2}	24.85	0.777	314.45	10.500	299.38	12.285	9.542
0$^{1\text{-}H2O}$	68.92	3.825	15.00	1.048	63.08	1.325	5.068
0$^{2\text{-}H2O}$	68.92	3.825	24.98	300.050	132.21	1.873	7.164
1^{H2O}	46.48	2.580	260.31	300.000	1136.03	7.141	18.425
2	100.00	4.991	1073.20	10.000	4207.68	41.792	208.56
3	100.00	4.991	648.63	1.000	3277.67	22.414	111.86
4	100.00	4.991	303.99	0.078	2606.06	8.091	40.378
5	100.00	4.991	39.73	0.077	2139.49	4.927	24.588
0^{SEC}	20118.75	1116.76	15	1.048	63.082	1.325	1479.43
1^{SEC}	20118.75	1116.76	15.03	6	63.704	1.334	1489.40
2$^{1\text{-}SEC}$	20218.75	1121.75	17.61	1.05	73.757	1.332	1493.89
2$^{2\text{-}SEC}$	20218.75	1121.75	15	1.048	62.841	1.331	1492.89
6	20201.54	1121.36	15	1.048	63.082	1.325	1485.52
7	20132.62	1117.53	15	1.048	63.082	1.325	1480.45
1^{PROD}	13.87643	0.770	15	1.048	63.082	1.325	1.020
1^{CCU}	17.207	0.391	15.0	1.048	28.290	18.844	7.368
2^{CCU}	17.207	0.391	311.9	25	311.30	30.478	11.916
3^{CCU}	17.207	0.391	95.0	24.998	83.054	26.593	10.397
4^{CCU}	17.207	0.391	211.9	80	183.45	30.666	11.990
5^{CCU}	17.207	0.391	45.0	79.998	-60.267	27.996	10.946
0$^{2\text{-}H2O'}$	46.48	2.58	24.98	300.05	132.21	1.873	4.832
0$^{2\text{-}H2O''}$	22.43689	1.2454	24.98	300.05	132.21	1.873	2.332
2^{H2O}	22.43689	1.2454	70.39	300.025	63.082	2.211	2.753
3^{H2O}	22.43689	1.2454	112.61	300	494.16	2.870	3.574

Table 5: Calculation results in characteristic stream points of negative-CO2 emission cycle with Syngas

Stream	$\dot{m}$ (g/s)	$\dot{n}$ (mol/s)	T (°C)	p (bar)	h (kJ/kg)	$\overline{e}^{tot}$ (kJ/mol)	$\dot{E}^{tot}$ (kW)
0$^{\mathbf{Fuel}}$	16.68	0.881	15.00	1.000	25.62	331.457	291.87
1$^{\mathbf{Fuel}}$	16.68	0.881	252.93	10.500	483.27	339.492	298.94
0$^{\mathbf{O2}}$	20.76	0.649	15.00	1.000	13.46	3.77	2.446
1$^{\mathbf{O2}}$	20.76	0.649	314.45	10.500	299.38	12.29	7.970
0$^{\mathbf{1\text{-}H2O}}$	62.56	3.473	15.00	1.048	63.08	1.325	4.600
0$^{\mathbf{2\text{-}H2O}}$	62.56	3.473	24.98	300.050	132.21	1.873	6.503
1$^{\mathbf{H2O}}$	42.00	2.331	281.84	300.000	1238.48	8.010	18.674
2	100.00	4.800	1077.40	10.000	4002.07	42.145	202.28
3	100.00	4.800	654.68	1.000	3103.15	22.675	108.83
4	100.00	4.800	310.60	0.078	2451.23	8.230	39.50
5	100.00	4.800	38.95	0.077	1986.59	4.918	23.61
0^{SEC}	19705.53	1093.82	15	1.048	63.082	1.325	1449.04
1^{SEC}	19705.53	1093.82	15.03	6	63.702	1.334	1458.81
2$^{1\text{-}SEC}$	19805.53	1098.62	17.48	1.05	73.199	1.334	1465.24
2$^{2\text{-}SEC}$	19805.53	1098.62	15	1.048	62.829	1.333	1464.33
6	19782.31	1098.09	15	1.048	63.082	1.325	1454.69
7	19719.75	1094.61	15	1.048	63.082	1.325	1450.09
1^{PROD}	14.22235	0.7895	15	1.048	63.082	1.325	1.046
1^{CCU}	23.218	0.5325	15.0	1.048	28.521	18.090	9.633
2^{CCU}	23.218	0.5325	314.5	25	314.97	29.759	15.85
3^{CCU}	23.218	0.5325	95.0	24.998	83.873	25.847	13.76
4^{CCU}	23.218	0.5325	212.6	80	185.62	29.937	15.94
5^{CCU}	23.218	0.5325	45.0	79.998	-53.004	27.317	14.55
0$^{2\text{-}H2O`}$	42	2.3314	24.98	300.05	132.21	1.873	4.366
0$^{2\text{-}H2O``}$	20.55952	1.1412	24.98	300.05	132.21	1.873	2.137
2^{H2O}	20.55952	1.1412	90.36	300.025	63.082	2.486	2.837
3^{H2O}	20.55952	1.1412	152.77	300	662.68	3.749	4.278

Key results for the two systems, both with methane and syngas as fuel, are listed in *Table 6*.

The net $\eta_{en,PDF0,net}$ and gross $\eta_{en,PDF0,gross}$ PFD0 process efficiency, and the net $\eta_{en,PDF1,net}$ and gross $\eta_{en,PDF1,gross}$ PFD1 cycle efficiency without capture were calculated according to

$$\eta_{\mathrm{en,gross}} = \frac{N_{\mathrm{GT1}} + N_{\mathrm{GT2}}}{\dot{Q}_{\mathrm{fuel}}} \tag{12}$$

$$\eta_{\mathrm{en,net}} = \frac{N_{\mathrm{net}}}{\dot{Q}_{\mathrm{fuel}}} = \frac{N_{\mathrm{GT1}} + N_{\mathrm{GT2}} - N_{\mathrm{C,O2}} - N_{\mathrm{C,fuel}} - N_{\mathrm{P}}}{\dot{m}_{\mathrm{fuel}} \cdot \mathrm{LHV}} \tag{13}$$

Table 6: Calculated main parameters of zero-CO_2 and negative-CO_2 gas power plant energy analysis with the use of Methane and Syngas

		Zero-CO_2 emission process		Negative-CO_2 emission cycle	
Parameter	**Unit**	**Methane**	**Syngas**	**Methane**	**Syngas**
Electrical power output*	kW	142.561	131.187	141.186	133.508
Combined turbine net power	kW	144.644	133.104	143.248	135.459
Power own needs without capture	kW	15.967	18.953	15.311	18.075
Power own needs with capture	kW	-	-	38.00	43.344
Chemical energy rate of combustion	kW	336.10	307.445	311.593	284.904
Fuel consumption	g/s	6.72	18.0	6.23	16.68
Net energy efficiency w.o. capture	%	43.03	43.29	45.97	47.55
Gross energy efficiency w.o. capture	%	47.78	49.45	50.88	53.88
Net energy efficiency w. capture	%	-	-	38.69	38.67
Gross energy efficiency w. capture	%	-	-	50.88	53.88
Net heat rate without capture	kJ/kWh	8365	8315	7830	7571
Gross heat rate without capture	kJ/kWh	7534	7280	7075	6681
Net heat rate with capture	kJ/kWh	-	-	9304	9309
Gross heat rate with capture	kJ/kWh	-	-	7075	6681
Exergy inflow*	kW	357.48	321.97	326.88	294.31
Exergy destruction*	kW	185.71	158.57	185.40	158.47
Exergy efficiency*	%	-	-	36.5	39.4

*(without oxygen separation)

The net efficiency of the PDF1 cycle with capture was determined as

$$\eta_{\text{en,net,w.c}} = \frac{N_{\text{net}}}{\dot{Q}_{\text{fuel}}} = \frac{N_{\text{GT1}} + N_{\text{GT2}} - N_{\text{C,O2}} - N_{\text{C,fuel}} - N_{\text{P}} - N_{\text{P,EC}} - N_{\text{C1,CO2}} - N_{\text{C2,CO2}}}{\dot{m}_{\text{fuel}} \cdot \text{LHV}} \tag{14}$$

where

$N_{\text{net}} = N_{\text{GT1}} + N_{\text{GT2}} - N_{\text{C,O2}} - N_{\text{C,fuel}} - N_{\text{P}}$ - combined turbine net power (kW)

$\dot{Q}_{\text{fuel}}$ - chemical energy rate of combustion (kW), rate of lower heating value

$N_{\text{own,w.o.c}} = N_{\text{C,O2}} + N_{\text{C,fuel}} + N_{\text{P}}$ - power own needs without capture (kW),

$N_{\text{own,w.c}} = N_{\text{C,O2}} + N_{\text{C,fuel}} + N_{\text{P}} + N_{\text{P,EC}} + N_{\text{C1,CO2}} + N_{\text{C2,CO2}}$ - power own needs with capture (kW).

The exergy efficiency of the PFD1 cycle (without taking into account the oxygen separation process) can be calculated as

$$\eta_{\text{ex}} = \frac{\dot{W}_{\text{net}}}{\dot{E}^{tot}_{0,\text{fuel}} + \dot{E}^{tot}_{0,\text{O2}}} = 1 - \frac{\dot{E}_{\text{d,proc}} + \dot{E}^{\text{tot}}_{1,\text{Prod}}}{\dot{E}^{tot}_{0,\text{fuel}} + \dot{E}^{tot}_{0,\text{O2}}} \tag{15}$$

In this expression, electric losses are not considered oxygen separation is drawn from the work rate, the O_2 is regarded as an inflow, while the net produced water is a discharge.

Results of the exergy analysis for system components are presented in Table 7 for PFD0. The net electric power output is what can be delivered when oxygen is separated. The inflow exergy is the sum of the total flow exergies of fuel (0^{Fuel}) and water ($0^{1\text{-}H2O}$), however not the O_2 inflow, since this is accounted as provided by the process. Work, exergy destruction and flow exergy are given as percentages of the fuel chemical exergy. The O_2 separation penalty is the exergy assumed used for the oxygen separation. The flow of pure O_2 is the benefit of this, represented by the chemical exergy of the O_2 stream. The remaining part of the penalty (86.8%, cf. Section 3.5) is then exergy destruction of the oxygen separation process.

Table 7: Results of exergy analysis. Work, exergy destruction and flow exergy in % of the fuel chemical exergy (mixing exergy included), PFD0

	Methane		**Syngas**	
	Rate (kW)	%fuel ch.ex	Rate (kW)	%fuel ch.ex
Exergy inflow	354.32	101.37	319.31	101.40
Net electric power output	122.58	35.07	114.91	36.49
Outflow exergy, Stream 5	29.31	8.38	34.02	10.80
Exergy destruction distribution:				
Combustor	162.85	46.59	140.79	42.22
Gas turbines	8.02	2.48	7.70	2.64
Compressors, pump	3.87	1.20	3.36	1.06
Heat exchanger HE	3.52	1.09	6.83	2.17
Electric and mech losses	7.45	2.30	7.73	2.65
O2 separation penalty	23.84	6.82	19.92	6.32

The exergy analysis of the negative CO2 emission power plant is shown inTable 8. Also here, the oxygen separation is included when the net electric output is evaluated. Furthermore, the inflow is the fuel, as oxygen and water flows are accounted as provided by the system. In addition, it can be mentioned that the heat exchangers HE1, HE3 and HE4 have exergy efficiencies in the range 40-71% for methane and 50-76% for syngas. The specifications of the compressors and gas turbines lead to exergy efficiencies in the range 92-93%, while 44% for the pumps. These exergy efficiencies are evaluated as the ratio of the desired exergy rate and the utilized exergy rate. For compressors and pumps, the work input is the utilized exergy, while the desired product is the exergy increase. For gas turbines, the input is the exergy difference of the flow, while work is the desired output. For a heat exchanger, the cold-side exergy increase is the service, while the input is the hot-side flow exergy decrease. For the combustor, the desired product is the exit flow exergy, and the input is the entering flow exergies.

Not unexpected, the combustor was the main source of exergy destruction, with about 42-45% of the fuel chemical exergy. This is more than for conventional gas turbine combustors, which are typically in a range around 35%. One reason for the higher exergy destruction is the stoichiometric conditions: The reactants and reaction product here deviate more from the ambient conditions. For conventional combustors the oxidizer is air, and a large excess of air also gives an exhaust with a high content of air gases. Another reason is the in-combustor evaporation of water. This implies heat transfer over a large temperature difference between the flame and liquid water evaporating at the saturation temperature of the combustor pressure. It can also be noted that the combustor outlet (turbine inlet) temperature chosen here is as high as the state-of-the-art gas turbines. This is due to the development context.

Table 8: Results of exergy analysis. Work, exergy destruction and flow exergy in % of the fuel chemical exergy (mixing exergy included), PFD1.

	Methane		Syngas	
	Rate (kW)	%fuel ch.ex	Rate (kW)	%fuel ch.ex
Exergy inflow	323.96	100.00	291.87	100.00
Net electric power output	96.38	29.78	89.77	30.74
Exergy of CO_2-rich outflow	10.95	3.38	14.55	4.98
Sum useful output	107.33	33.16	104.32	35.72
Exergy, water discharge	1.02	0.32	1.05	0.36
O2 separation penalty	22.11	6.83	18.47	6.32
Exergy destruction distribution:				
Combustor	146.39	45.23	123.30	42.22
Gas turbines	8.02	2.48	7.70	2.64
Compressors, pumps	3.87	1.20	4.01	1.37
Heat exchangers HE1, HE3, HE4	3.52	1.09	2.92	1.00
Spray-ejector condenser	22.59	6.98	19.62	6.72
Heat exchanger HE2	1.00	0.31	0.91	0.31
Electric and mech losses	7.45	2.30	7.73	2.65

The spray-ejector condenser (with pump and throttle) is the second largest contribution to exergy destruction. It can be noted that the mass of injected water is quite large, about 200 times that of the flue gas. Even modest specific penalties of pumping and throttling will become notable when the flow rate is considered.

Oxygen separation has ha relatively high cost in form of exergy. This is here treated as a separate process and based on literature data. Finding a more efficient separator will directly reduce the penalty and increase the efficiency.

Furthermore, the chemical exergy of the captured CO_2 represents 3.3% of the fuel chemical exergy for syngas, while 2.2% for methane. This is the thermodynamic value of the capture. In addition, the CO_2 rich flow is delivered at an elevated pressure (here, 80 bar) for further transportation to storage. Capture and compression inevitably reduce the power output. On the other hand, the capture and storage are a desired product of the process, and the exergy therefore is accounted as useful or product exergy of the plant.

Further work with the negative CO_2 power plant will include scrutinizing the exergy destruction sources. Any reduction of irreversibility can increase the useful output.

5 Conclusions

The energy analysis of developed cycles helps to calculate the performances by the main cycle parameters of the negative-CO_2 power plant and to evaluate the CO_2 emission levels, which are as follows: for PFD0 CO_2 emission is around 460 kg/MWh where the fuel is methane, and 0 kg/MWh when syngas is used. In negative-CO_2 emission cycle PFD1, the CO_2 emission is equal to 0 when the methane is main fuel. Around 510 kg/MWh is captured thanks to the oxy-combustion with water and subsequent condensing of water from the CO_2. When the fuel is syngas coming from the sewage sludge gasification process, the negative CO_2 emission reaches a value of 740 kg/MWh.

The exergy analysis of the systems previously studied by energy analysis quantifies the thermodynamic losses and the flows of exergy. For the syngas-fueled negative CO_2 emission cycle, the net electric power is 30.7% of the fuel chemical exergy. Another 5.0% represented the captured and compressed CO_2-rich flow, which is also a useful and desired product of the process. The penalty of using O_2 for combustion is evaluated on the basis of literature data to 6.3% of the supplied fuel chemical exergy.

The main sources of exergy destruction were the wet combustion chamber (42.2%) and the spray ejection condenser (6.7%). Each of the other system components had lesser contributions to the exergy loss. The same system fueled with methane had similar values for useful and destructed exergy. The discussion indicates on potential measures for improving the process.

Acknowledgments: The research leading to these results has received funding from the Norway Grants 2014-2021 via the National Centre for Research and Development. Article has been prepared within the frame of the project: "Negative CO2 emission gas power plant" - NOR/POLNORCCS/NEGATIVE-CO2-PP/0009/2019-00 which is co-financed by programme "Applied research" under the Norwegian Financial Mechanisms 2014-2021 POLNOR CCS 2019 - Development of CO2 capture solutions integrated in power and industry processes.

6 References

[1] https://nco2pp.mech.pg.gda.pl/pl - Negative CO2 emission gas power plant

[2] Ziółkowski, P., Madejski, P., Amiri, M., Kuś, T., Stasiak, K., Subramanian, N., Pawlak-Kruczek, H., Badur, J., Niedźwiecki, Ł., Mikielewicz, D. (2021), Thermodynamic Analysis of Negative CO2 Emission Power Plant Using Aspen Plus, Aspen Hysys, and Ebsilon Software. *Energies*, **14**, 6304. https://doi.org/10.3390/en14196304

[3] Ganjehkaviri, A., Mohd Jaafar, M. N., Ahmadi, P., Barzegaravval, H. (2014) Modelling and optimization of combined cycle power plant based on exergoeconomic and environmental analyses. *Appl. Therm. Eng.* **67** (1–2), pp. 566–578. https://doi.org/10.1016/j.applthermaleng.2014.03.018

[4] Mokhtari, H., Ahmadisedigh, H., Ameri, M. (2017) The optimal design and 4E analysis of double pressure HRSG utilizing steam injection for Damavand power plant. *Energy* **118**, pp. 399–413. https://doi.org/10.1016/j.energy.2016.12.064

[5] Ziółkowski, P., Kowalczyk, T., Lemański, M., Badur, J. (2019). On energy, exergy, and environmental aspects of a combined gas-steam cycle for heat and power generation undergoing a process of retrofitting by steam injection. *Energy Convers. Manage.* **192**, pp. 374–384. https://doi.org/10.1016/j.enconman.2019.04.033

[6] Cassetti, G., Rocco, M. v., Colombo, E. (2014). Exergy based methods for economic and risk design optimization of energy systems: Application to a gas turbine. *Energy* **74**(C), pp. 269–279. https://doi.org/10.1016/j.energy.2014.07.043

[7] Soufi, M. G., Fujii, T., Sugimoto, K. (2004). A modern injected steam gas turbine cogeneration system based on exergy concept. *Int. J. Energy Resear.* **28**(13), pp. 1127–1144. https://doi.org/10.1002/er.1019

[8] Amrollahi, Z., Ertesvåg, I.S., Bolland, O. (2011) Optimized process configurations of post-combustion CO2 capture for natural-gas-fired power plant-Exergy analysis, *Int. J. Greenhouse Gas Control* **5**, pp. 1393–405. https://doi.org/10.1016/j.ijggc.2011.09.004.

[9] Mondino, G., Spjelkavik, A. I., Didriksen, T., Krishnamurthy, S., Stensrød, R. E., Grande, C. A., Nord, L. O., Blom, R. (2020). Production of MOF Adsorbent Spheres and Comparison of Their Performance with Zeolite 13X in a Moving-Bed TSA Process for Postcombustion CO2 Capture. *Ind. Eng. Chem. Resea.* **59**(15), 7198–7211. https://doi.org/10.1021/acs.iecr.9b06387

[10] Ertesvåg, I.S., Kvamsdal, H.M., Bolland, O. (2005) Exergy analysis of a gas-turbine combined-cycle power plant with precombustion CO_2 capture, *Energy* **30**, pp. 5–39. https://doi.org/10.1016/j.energy.2004.05.029.

[11] Mohammadpour, M., Houshfar, E., Ashjaee, M., Mohammadpour, A. (2021). Energy and exergy analysis of biogas fired regenerative gas turbine cycle with CO2 recirculation for oxy-fuel combustion power generation. *Energy* **220**. https://doi.org/10.1016/j.energy.2020.119687

[12] Okeke, I. J., Ghantous, T., & Adams, T. A. (2021). Design strategies for oxy-combustion power plant captured CO2 purification. *Chem. Prod. Proc. Mod.* https://doi.org/10.1515/cppm-2021-0041

[13] Fu, C., Gundersen, T., (2012) Using exergy analysis to reduce power consumption in air separation units for oxy-combustion processes, Energy 44, pp. 60-68. https://doi.org/10.1016/j.energy.2012.01.065

[14] Ziółkowski, P., Badur, J., Pawlak-Kruczek, H., Stasiak, K., Amiri, M., Niedźwiecki, Ł., Krochmalny, K., Mularski, J., Madejski P., Mikielewicz, D. (2022) Mathematical modelling of gasification process of sewage sludge in reactor of negative CO_2 emission power plant, *Energy,* **244(pt. A)**, art. no. 122601, pp. 1–16. https://doi.org/10.1016/j.energy.2021.122601

[15] Steag Energy Services Ebsilon®Professional 15.00. Available online: https://www.ebsilon.com/

[16] Soave, G. Equilibrium constants from a modified Redlich-Kwong equation of state. Chem.Eng. Sci., 27, 1197-1203. https://doi.org/10.1016/0009-2509(72)80096-4

[17] International Association for the Properties of Water and Steam. IAPWS R7-97(2012) http://www.iapws.org/relguide/IF97-Rev.html

[18] Ertesvåg I.S. (2007), Sensitivity of chemical exergy for atmospheric gases and gaseous fuels to variations in ambient conditions, *Energy Convers. Manage.*, **48(7)**, pp. 1983-1995, https://doi.org/10.1016/j.enconman.2007.01.005

[19] Szargut J., Morris DR., Steward FR. (1998), Exergy analysis of Thermal, chemical, and metallurgical processes. Hemisphere, 1988